Conference Proceedings

Solar World Congress 2015
Daegu, Korea, 08 – 12 November 2015

Study on amorphous Silicon single junction p-i-n PV cell

Al-Rajib Bhuiyan and Himangshu Ranjan Ghosh

Institute of Energy, University of Dhaka, Dhaka-1000, Bangladesh

Abstract

The performance of solar PV cells depends on its design, material properties and fabrication technology. In this study design and analysis on thin film single junction hydrogenated amorphous silicon (aSi:H) has showed that the efficiency of a single junction PV cell can be achieved upto 9.823% for with optimized window layer bandgap of 1.85eV. For this the current density is 13.827 mA/cm2, open circuit voltage is 0.987 volts and fill factor is 0.719. Moreover different interface recombination velocities are applied to investigate the impacts on short-circuit current density (Jsc), open-circuit voltage (Voc), fill factor (FF) and efficiency ( ). Higher recombination velocity of front and back contact give a detrimental impact on Jsc& . Jsc and drastically decline in the range where surface recombination speed are greater than 104 cm/s. it would be possible to yield efficiency more than 10% by reducing surface recombination speed from 107 cm/s to 104cm/s. The Quantum Efficiency (QE) curve has revealed that the cell has good spectral response in the wavelength range 0.4 μm – 0.65 μm which means that it would be a good candidate as a top cell of double junction/ micromorph solar cell configuration and as a middle cell in triple junction structure. The research has been carried out with AMPS-1D modelling and computer simulation program.

Keywords: *Thin film solar cell, Amorphous silicon solar cell*

1. Introduction

Amorphous silicon (aSi:H) technology was up to now the only thin film concept, that has entered into large scale production plants in turning out about 5MW/y. But already now aSi:H modules are sold at lower prices than wafer based crystalline silicon modules. However, compared to crystalline silicon the efficiency of commercially available aSi:H solar cell module suffer still from relative low efficiency. While in the research laboratory stabilized efficiencies over 13% have been demonstrated for small size cells. There is a gap between this record test cells and the translation into commercial modules. It is interesting to look into the various individual factors that cause efficiency losses for aSi:H technology between laboratory records cell and industrial production (Fonash, 2010).

The performance of solar photovoltaic cells depends on its design, material properties, and fabrication technology. Photovoltaic (PV) researchers present improved cells over the period of time, although the overall process is quite complex, expensive, and time consuming. Numerical simulation is the best approach for solar cell researchers, which help to find out an optimized structure with good fitted parameters. As a result fabrication complexity, costs, and time reduce significantly. The major objectives of numerical modeling and simulation in solar cell research are testing the validity of proposed physical structures, geometry on cell performance, and fitting of modeling output to experimental results. The numerical modeling has become indispensable tools for designing a high-efficiency solar cell. Numerical modeling is increasingly used to obtain insight into the details of the physical operation of thin-film solar cells. Over the years, several modeling tools specific to thin-film PV devices have been developed. A number of these tools have been reached in a mature status and are available to the PV community. In this study AMPS-1D simulation software (AMPS 1D 2015) has been used.

doi:10.18086/swc.2015.05.07 Available at http://proceedings.ises.org

2. Methodology

AMPS can simulate an extremely general semiconductor device structure. In the electrical part of the model, three coupled differential equations: the Poisson's equation and the two carrier continuity equation are solved simultaneously under non-equilibrium steady state conditions (i.e., under the effect of voltage or light bias, or both) by using the method of finite differences and Newton-Raphson technique, directly from the first principles (Belfar et al. 2011). The equations used are:

Poisson's Equation:

$$\frac{\partial^2 \psi(x)}{\partial^2 x} = \frac{\rho(x)}{\varepsilon} \qquad \text{(eq. 1)}$$

Hole Continuity equation:

$$G(x) - R(p(x), n(x)) - \frac{1}{q}\frac{\partial J_p(x)}{\partial x} = 0 \qquad \text{(eq. 2)}$$

Electron Continuity equation

$$G(x) - R(p(x), n(x)) + \frac{1}{q}\frac{\partial J_n(x)}{\partial x} = 0 \qquad \text{(eq. 3)}$$

Where $\rho(x)$ is the charge density

$$\rho(x) = q[p(x) - n(x) + p_T(x) - n_T(x) + N_{net}^{+}] \qquad \text{(eq. 4)}$$

And the electric field

$$E = \frac{\partial \psi(x)}{\partial x} \qquad \text{(eq. 5)}$$

where, ε is the dielectric constant,
E the electrostatic field, represents the position in energy of the local vacuum level,
x the position in the device,
p and n the valence-band hole density and the conduction band electron density, respectively,
q the electronic charge,
R the recombination rate,
p_T and n_T the trapped hole and electron population density, respectively,
N_{net}^{+} the net doping density, if any,
G the electron-hole pair generation rate,
$J_p$andJ_n the hole and electron current density respectively and
E_{FP} and E_{F},, the hole and electron quasi Fermi levels.

In this study, the three state variables that completely define the state of a device have been taken to be the local vacuum level, ψ and the quasi-Fermi levels E_{FP} and E_{Fn}. Once these three dependent variables are known as a function of x, all other information about the system can be determined as functions of position. In thermodynamic equilibrium, the Fermi level is a constant as a function of position and hence the three Equation (1-3) essentially reduce to only one equation viz., the Poisson's equation. Therefore, the local vacuum level $\psi(x)$ is the only unknown to be solved for in thermodynamic equilibrium.

In the non-thermodynamic equilibrium steady-state, a system of three coupled non-linear second order differential equations in the tree unknown (ψ, E_{Fn}, E_{Fp}) are obtained, In order to solve these equations for state variables (ψ, E_{Fn}, E_{Fp}), we need six boundary conditions, two for each dependent variable. The first

two boundary conditions are modified versions of the ones used for solving Poisson's equation in thermodynamic equilibrium:

$$\psi(0) = 0 - \chi(L) - \varphi_{bL} + \varphi_{bO} - \chi(0) - V \qquad \text{(eq. 6)}$$

And

$$\psi(L) = 0 \qquad \text{(eq. 7)}$$

Where, L is length of the device,

$\chi(0), \chi(L)$ are the electron affinities at x = 0 and x = L, respectively and

V is the applied voltage.

The zero of $\psi = \psi(x)$ is generally chosen to be the position in energy of the vacuum level at the boundary point x = L. The boundary conditions for the Poisson's equations in thermodynamic equilibrium are Equation 6 with the applied voltage V term absent and Equation 7. The four other boundary conditions are obtained from imposing constraints on the currents at the boundaries at x = 0 and x =L. These constraints force the mathematics to acknowledge the fact that the currents must cross at x = 0 and x = L (the contact positions) by either thermo ionic emission or interface recombination. Expressed mathematically, we obtain the following:

$$J_n(0) = qS_{n0}[n(0)-n_0(0)] \qquad \text{(eq. 8)}$$
$$J_p(0) = qS_{p0}[p(0)-p_0(0)] \qquad \text{(eq. 9)}$$
$$J_n(L) = qS_{nL}[n(L)-n_0(L)] \qquad \text{(eq. 10)}$$
$$J_p(L) = qS_{pL}[p(L)-p_0(L)] \qquad \text{(eq. 11)}$$

Where, S_{n0}, S_{p0} are surface recombination velocities for electrons and holes respectively at the x = 0 interface and quantities

S_{nL}, S_{pL} are the corresponding velocities at the x = L interface.

The largest Value the can have is $\approx 10^7$ cm sec^{-1} dictated by thermionic emission. Here, n(0) (p(0)) are the electron (hole) density at x =0, n(L) (p(L)) are the same at x = L.

$N_0(0)$ ($p_0(0)$), $n_0(L)$ ($p_0(L)$) are the electron (hole) density in the thermodynamic equilibrium at x = 0 and x = L, respectively. With the help of the boundary conditioned stated above; the three Eq. 1 to 3 can be solved simultaneously for $\psi = \psi(x)$, $E_{fn} = E_{fp}$ (x) and $E_{Fp} = E_{Fp}(x)$. For this, the different terms in the equations are to be calculated first. The gape states and two Gaussian distribution functions to simulate the dangling bond states. The generation term in the continuity equations has been calculated using a semi empirical model (Leblanc et al., 1994) that has been integrated into the modelling programme. Both specular interference effects and diffused reflectance and transmittances due to interface roughness were taken into account.

3. Data and Result

Figure 1 gives the dark and light J-V characteristics of simulated aSi:H (p-i-n) single junction solar cell as calculated on the basis of model AMPS-1D. The calculated light J-V characteristics of the cell yield the following results:

Short circuit current density of Jsc= 13.827 mA/cm2,
Open circuit voltage Voc = 0.987 volt,
Fill-factorFF = 0.719,
Efficiency = 9.823 %.

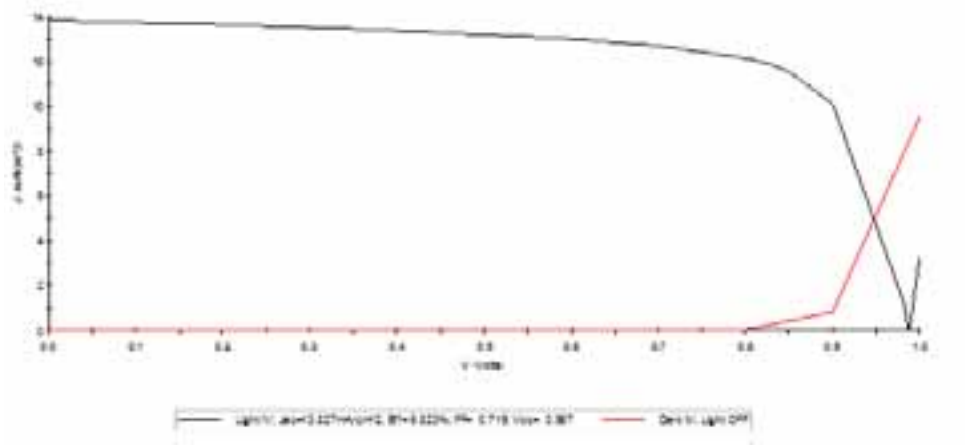

Fig. 1: Simulated J-V Characteristics curve of single junction (pin) aSi:H solar cell

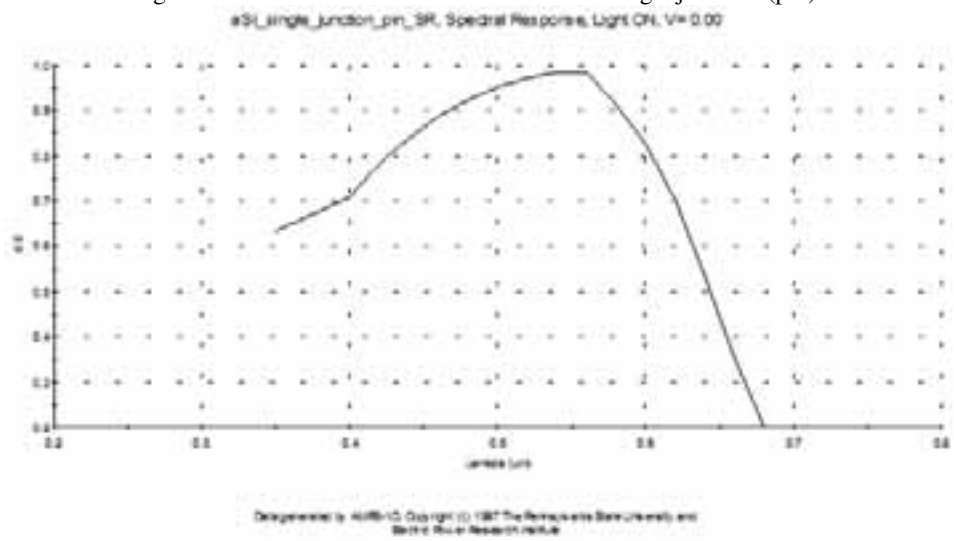

Fig. 2: Spectral response curve of single junction (pin) aSi:H solar cell

Figure 2 shows the quantum efficiency (QE) under AM1.5 illumination at 0 volts. From this SR curve it is clear that due to higher bandgap of aSi:H silicon, it has spectral response only below wavelength of 700nm. With respect to a band gap of 1.85 eV theband gap utilization is relatively low dueto the high levels of SRH recombination andthe relative broad valence and conduction-band tails.

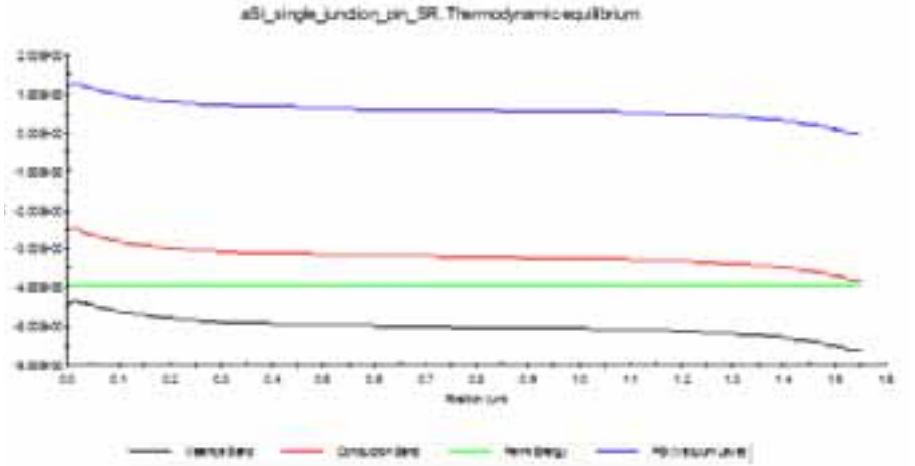

Fig. 3:Thermal equilibrium band diagram of aSi:H single junction solar cell

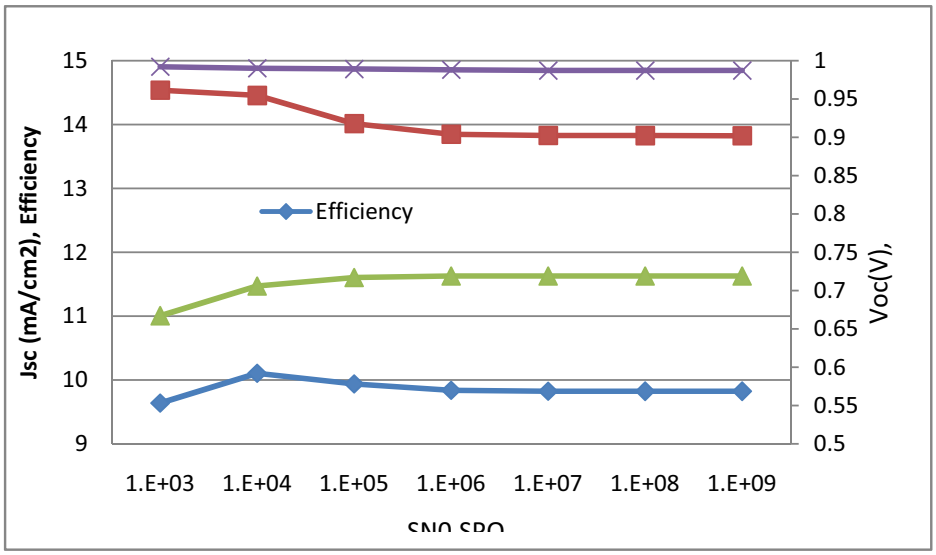

Fig. 4: Impacts on Voc, Jsc, FF& Eff come from the interface recombination speed

Interface recombination is one of the important recombination models. Different interface recombination velocities were applied to investigate the impacts on short-circuit current density (J_{sc}), open-circuit voltage (V_{oc}), fill factor (FF) and efficiency (Eff). The results are shown in Figure 5. In this simulation, the Rs mainly depends on thematerial properties, such as the interface recombination velocity, and whether the defects exist or not. Assume that the square of this solar cell is unity square centimeter. From Figure 4, it can be seen that Jsc and Eff drastically decline in the range where SNO and SPO are greater than 10^4 cm/s. The reason is that the increase in interface recombination velocity reduces the number of holes and electrons collected by the electrodes so that the short-circuit current reduces. Experimentally, the SNO, SPO, should be controlled into small value by optimizing the conditions of material growth in order to improve the conversion efficiency.

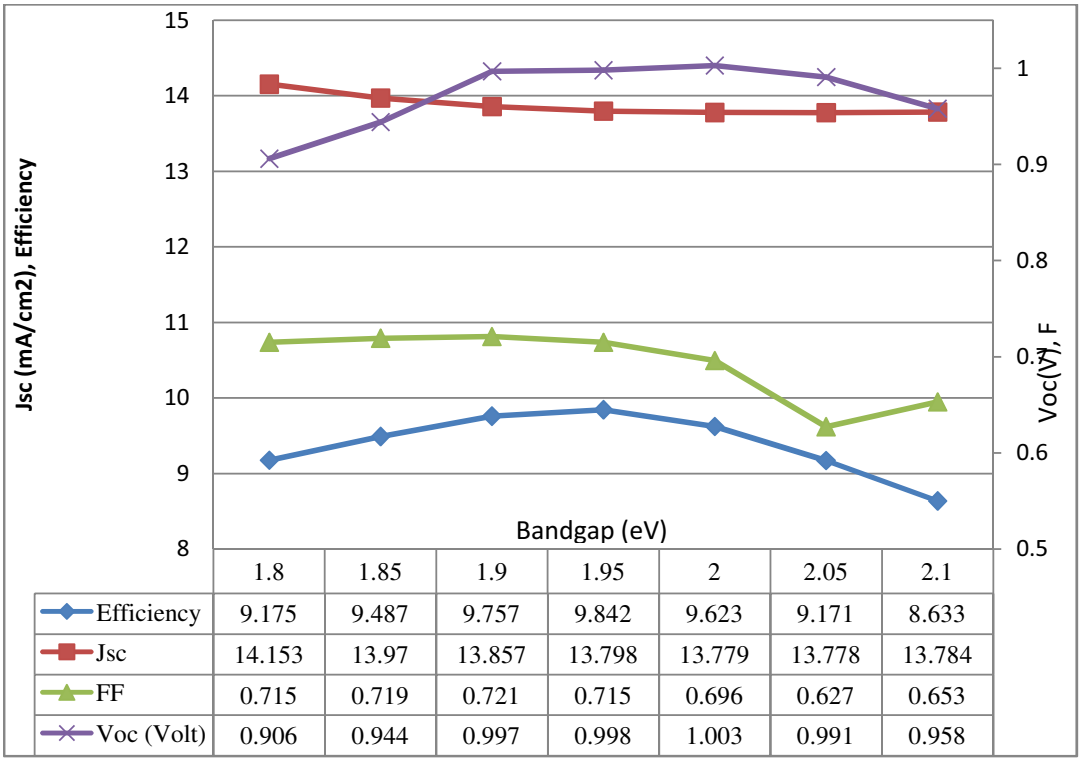

	1.8	1.85	1.9	1.95	2	2.05	2.1
Efficiency	9.175	9.487	9.757	9.842	9.623	9.171	8.633
Jsc	14.153	13.97	13.857	13.798	13.779	13.778	13.784
FF	0.715	0.719	0.721	0.715	0.696	0.627	0.653
Voc (Volt)	0.906	0.944	0.997	0.998	1.003	0.991	0.958

Fig. 5: Impacts on Voc, Jsc, FF& Eff come from the Window layer bandgap

Figure 5 gives the impacts on V_{oc}, J_{sc}, FF & Efficiency come from the window layer bandgap. From this figure it can be seen that the maximum efficiency of 9.82% has been achieved for window layer bandgap at 1.95 eV. Before and after the bandgap of 1.95 eV the efficiency decreases sharply due to decrease of photoconductivity and photosensitivity.

4. Conclusion

Win AMPS-1D simulation software, the best efficiency of this numerically designed single junction aSi:H solar cell is 9.823% with intrinsic layer thickness of 1200 nm and optimum window layer bandgap of 1.85eV. The obtained results show that the interface recombination speeds of front and back contact is crucial to short circuit current density and efficiency of aSi:H solar cell. Therefore one can increase the performance of aSi:H solar cell by minimizing the surface recombination speed of transparent conducting oxide. The Quantum Efficiency (QE) curve shows that the cell has good spectral response in the wavelength range 0.4 µm – 0.65 µm which means that it would be a good candidate as a top cell of double junction/ micromorph solar cell configuration and as a middle cell in triple junction structure.

5. References

Analysis of Microeletronic and Photonic Structures - AMPS-1D, 2015. *www.**amps**modeling.org/latest.html*

Belfar Abbas and Mostefaoui Rachida, 2011. Simulation of n_1-p_2 Microcrystalline Silicon Tunnel Junction with AMPS-1D in a-Si :H/µc-Si :H Tandem Solar Cells. *Journal of Applied Sciences, 11: 2932-2939.*

Fonash Stephen, 2010. Solar Cell Device Physics, 2nd Edition, Academic Press

Leblanc, F., J. Perrin and J. Schmitt, 1994. Numerical modeling of the optical properties of hydrogenated amorphous-silicon-based pin solar cells deposited on rough transparent conducting oxide substrates. J. Appl. Phys., 75: 1074-1087.